3D RAPLICASOL model of simultaneous ICRF FW and SW propagation in ASDEX Upgrade conditions

M. Usoltceva[1,2,3,a)] W. Tierens[1], A. Kostic[1,2], J-M. Noterdaeme[1,2], R. Ochoukov[1] and W. Zhang[1]

[1]*Max-Planck-Institut für Plasmaphysik, Boltzmannstr. 2, 85748 Garching, Germany*
[2]*Department of Applied Physics, Ghent University, 9000 Ghent, Belgium*
[3]*IJL, Université de Lorraine, 54011 Nancy, France*

[a)]Corresponding author: mariia.usoltceva@ipp.mpg.de

Abstract. A 3D RAPLICASOL model is presented where simultaneous propagation and absorption of both the FW and the SW is achieved. The modelling conditions are relevant for experimental conditions in ASDEX Upgrade (AUG) tokamak, magnetic field of 2 T, gas mixture of 98.5% D + 1.5% H, ICRF (Ion Cyclotron Range of Frequencies) antenna frequency of 36.5 MHz, opposite phasing on the 2 straps and coupled power of 1 MW. A radial density profile from EMC3-Eirene simulations is used. The antenna geometry is simplified in the poloidal direction and the plasma parameters variations are taken into account only partially. In principle, the methods presented here are applicable to models with the full scale of complexity. Up to now, the SW propagation was avoided in simulations of the ICRF waves for tokamaks, usually by artificial density modification (vacuum layer) near the antenna strap. The importance of the SW as a source of electric fields and ICRF power deposition in the edge plasma is highlighted by this work.

1. INTRODUCTION

Numerical 3D simulations of the ICRF waves propagation are a powerful tool for the prediction of field distributions and for the optimization of the antenna design. Some of the developed modelling tools as RAPLICASOL or TOPICA [1] have succeeded in simulating the fast wave (FW) mode of the ICRF waves launched by accurate 3D models of tokamak antennas. The SW propagates at lower densities than the FW, mostly behind the leading edge of the antenna limiters. The SW does not contribute to the heating of the core plasma and its simulation is always complicated by numerical issues because of the Lower Hybrid (LH) resonance presence. As a result, the SW propagation and the fields excited have been consistently excluded from simulations and moreover the ICRF power dissipation by this mode to the particles of the edge plasma has been neglected. The recent work done on the modelling of the SW led to significant improvements in its understanding [2]. Two important aspects need to be taken into account for the SW modelling, the antenna strap must be inserted in the plasma (no vacuum layer) and the collisions should be accounted for. Many of the previous unsuccessful attempts to simulate the SW are thought to be caused by the failure to complete these two necessary steps. Following the possibility to simulate the SW, it became feasible to model both propagating ICRF wave modes together. The calculations in this paper are done for the conditions relevant to the ICRF 2-strap antennas of the AUG tokamak. As shown below, the field strength and the power absorption of the two modes can be compared. Significant collisional power absorption of the SW will be demonstrated and the deficiency of the collisionless approach will be explained.

2. MODEL DESCRIPTION

In the cold plasma approximation [3] there are two solutions of the wave equation. They can be written in a simplified form that is valid under certain conditions:

$$n_{\perp FW}^2 = \frac{(\varepsilon_R - n_\parallel^2)(\varepsilon_L - n_\parallel^2)}{(\varepsilon_\perp - n_\parallel^2)}, \text{ when } |\varepsilon_\parallel| \gg |n_{\perp FW}^2|, |\varepsilon_\parallel| \gg |n_\parallel^2|, |\varepsilon_\perp|, |\varepsilon_X| \text{ and } \varepsilon_\perp \neq n_\parallel^2 \quad (1)$$

$$n_{\perp SW}^2 = \varepsilon_\parallel \left(1 - \frac{n_\parallel^2}{\varepsilon_\perp}\right), \quad \text{when } |\varepsilon_\parallel| \approx |n_{\perp SW}^2|, |\varepsilon_\parallel| \gg |n_\parallel^2|, |\varepsilon_\perp|, |\varepsilon_X| \text{ and } \varepsilon_\perp \neq n_\parallel^2 \quad (2)$$

Here ε_* are the Stix parameters defined in [3], $\boldsymbol{n} = \boldsymbol{k}c/\omega$ is the refraction index, $\boldsymbol{k}$ is the wave vector, c is the speed of light and $\omega = 2\pi f$ is the angular frequency of the ICRF wave. For simplicity, the magnetic field $\boldsymbol{B}$ is taken to be parallel to z and the y-component of the wave vector is assumed to be zero, so that $\boldsymbol{n} = n_\perp \boldsymbol{x} + n_\parallel \boldsymbol{z} + 0 * \boldsymbol{y}$.

The ICRF waves propagation is studied in this work under conditions relevant to H-mode experiments in AUG. The ICRF antenna and plasma parameters are: f = 36.5 MHz, opposite phasing on the 2 straps, $k_\parallel$ = 8.98 rad/m, coupled power P_{cpl} = 1 MW, B = 2 T, gas mixture: 98.5% D + 1.5% H. The radial variation of the B-field is neglected. The geometry of the AUG antenna #1 has been simplified. A cut in the toroidal-radial plane of the full 3D geometry was taken and extended vertically (Fig. 1), so that all poloidal inhomogeneities of the realistic antenna are ignored except the coaxial feeding lines. At the same time the straps and the limiters shape and all gaps between them are reproduced with high precision (visible on a top view, Fig. 3-5). The precise geometry plays a crucial role because of the small characteristic length of the wave field in the vicinity of the straps and the limiters.

The FW and the SW behaviour is plotted in Fig. 2 as a function of radius (along x axis) for the AUG parameters described above (conditions in (1) and (2) remain valid). Positive y axis values correspond to regions of the wave propagation. A 1D density profile from EMC3-Eirene [4] simulations was used and averaged poloidally and toroidally. The radial density profile is shown in the same figure and it can be seen that the EMC3-Eirene data was used only partially, from the limiter leading edge (r = 0.175 m) to r = 0.225 m and was further extrapolated as a constant. In the limiter shadow the density profile was changed to a much steeper one which should better represent the experimental conditions. The density was made constant near the straps (r = 0.095 – 0.115 m), otherwise the solution convergence was not possible (direct solver). The volume where r < 0.02 m is filled with vacuum, since in the experiment very low densities are expected in close proximity of the coaxial lines and inside them. The density is radially constant inside the domain with perfectly matched layer (PML) (r > 0.27 m), a material which absorbs the incoming wave power, so nothing is reflected back to the plasma. On the sides (in z direction) PML domains are also placed, with the same radial density distribution as in Fig. 2. The modelling was performed in RAPLICASOL (based on COMSOL) [1] where the described above analytical equations are introduced manually into the model.

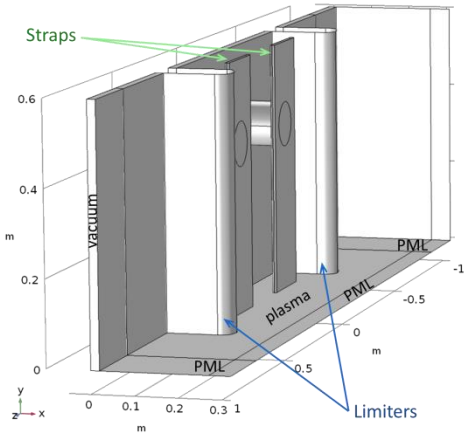

FIGURE 1. The simplified AUG 2-strap antenna geometry, with indicated domain materials

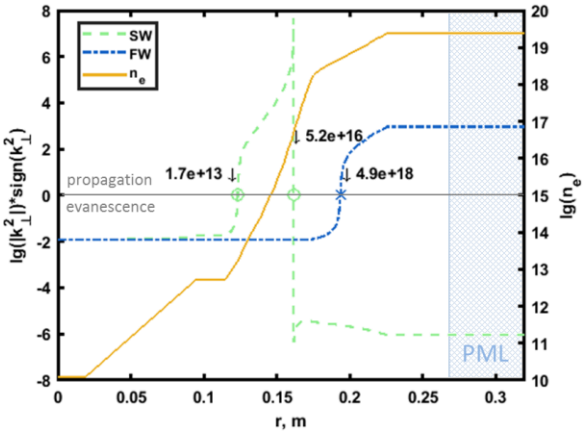

FIGURE 2. FW and SW propagation as a radial function; density radial profile in lg scale

In order to successfully simulate the SW, its special properties must be taken into account, which differ significantly from the FW properties. The SW, due to the signs of the dielectric tensor coefficients, is a hyperbolic wave in the propagation region [2] (parameter space relevant to ICRF antennas in fusion plasma experiments). The hyperbolic wave front of the SW does not propagate spatially in the direction of $\boldsymbol{k}$ but remains at a constant location. The wave field is concentrated in a small region of a resonance cone (RC), which angle to the magnetic field α is defined by the direction of $\boldsymbol{k}$ and depends on the density. The characteristic size of the RC that needs to be resolved in numerical modelling is the transverse size of the cone along $\boldsymbol{k}$ [2]. It is defined by the wave excitation source, i.e. the current density distribution on the antenna strap or the image currents on the limiters. The RC width along the magnetic field is conserved and is equal to the excitation source width, and consequently the transverse size is very

small at small α. Additional numerical difficulties appear when introducing a sharp density jump from vacuum to plasma where the SW propagates [2]. In the present work the mesh was made fine enough to resolve the change in the RC angle with the radius (Fig. 3) and the plasma domain was placed around the strap without a vacuum layer which ensured that the SW correct propagation was modelled. In Fig. 3-5 the blue line indicates the FW cut-off and the green lines show the radial positions of the SW cut-off and resonance according to Fig. 2.

The principal issue of the field singularity at the LH resonance vanishes in the presence of collisions. The electric field at the resonance location becomes finite and it is very small compared to the field inside the RC due to the nature of the RC propagation [2]. Only the dominant electron-neutral collisions (frequency ν_{en}) are considered in the present simulations. The collisions were implemented into our COMSOL model by following replacements for the electron Larmor frequency Ω_{ce} and the electron plasma frequency ω_{pe} [5]:

$$\Omega_{ce} \to \Omega_{ce}\frac{1}{1-i(\nu_{en}/\omega)};\ \omega_{pe} \to \omega_{pe}\frac{1}{1-i(\nu_{en}/\omega)} \quad (4)$$

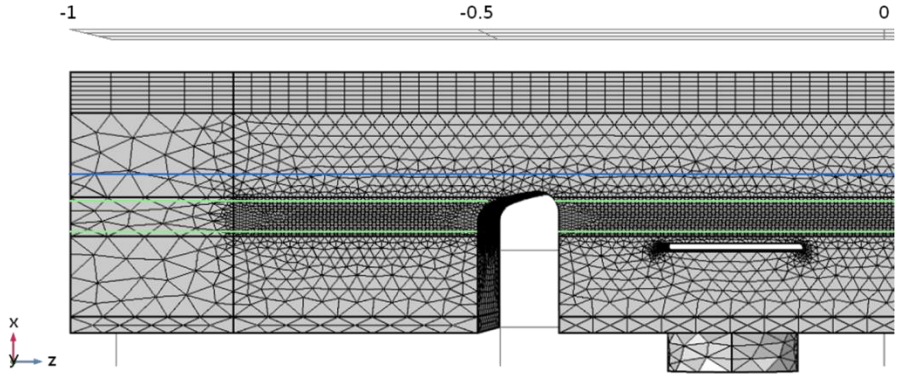

FIGURE 3. Mesh used in the simulation, top view, only one half of the box shown (symmetric for the other half)

3. SIMULATION RESULTS

The modelling was performed at the plasma conditions described in the Section 2 and with radially constant ν_{en}= 10^6 Hz $< \omega$. The results can be seen in Fig. 4. The strongest field component E_x (radial) is plotted. The FW field is much weaker than the SW field and not visible in Fig. 4a. To show the propagating FW a shortened color scale range is used (Fig. 4b). The rapid radial growth of $k_\perp$ (at constant $k_\parallel$) from 0 at the SW cut-off to very high values even before the LH resonance is observed by looking at the RC angle to the magnetic field. Since the $k_\parallel$ component is small relative to $k_\perp$ for most of the SW propagation region, the resulting k is directed nearly perpendicularly to B, hence the RC wave front extends almost parallel to the magnetic field. Multiple reflections from the limiters in close proximity to the straps and rather weak collisional damping lead to the field of the SW being significantly large near the LH resonance layer. This situation is different from multiple examples in [2], where the strong RC field was present only at considerable distance from the LH resonance. Nevertheless, due to collisional term, there is no singularity at the resonance, so the LH resonance presence does not lead to any significant numerical disturbance neither in the SW, nor in the FW. With the current conditions of the model, the SW field consists of numerous RCs, excited both by the strap current and by the limiters image currents. Each RC bounces between the metallic walls with very small incident angle, creating a complex field structure with multiple overlapping. The toroidal size of the RCs is defined here by the mesh size and it will be the case independent of the further mesh refinement. The continuous evanescent field in the layer before the SW cut-off defines the profile of the RC field in z direction. Numerical discretization inevitably introduces some disturbance, which an RC wave is very sensitive to.

The model including both the FW and the SW allows calculating the percentages of the power coupled to the plasma by each mode. The power dissipation density, plotted in Fig. 5 on one poloidal cut, is a value calculated by COMSOL at each point of the simulation space. The power absorption for the two ICRF modes is clearly spatially isolated – the SW is absorbed by collisions and a part of the side PMLs radially corresponding to the SW propagation, while the FW is absorbed in the front PML and in the side PMLs where the densities are high enough for the FW propagation. Therefore, the total amount of the power absorbed can be integrated in the domains and for this model the result is 9 % for the SW and 91 % for the FW. A calibration of the absolute values of the resonance circuit elements parameters and the input power as well as more precise collisional frequency values would allow predicting the absolute values of the power coupled to the plasma by each wave mode and its spatial distribution.

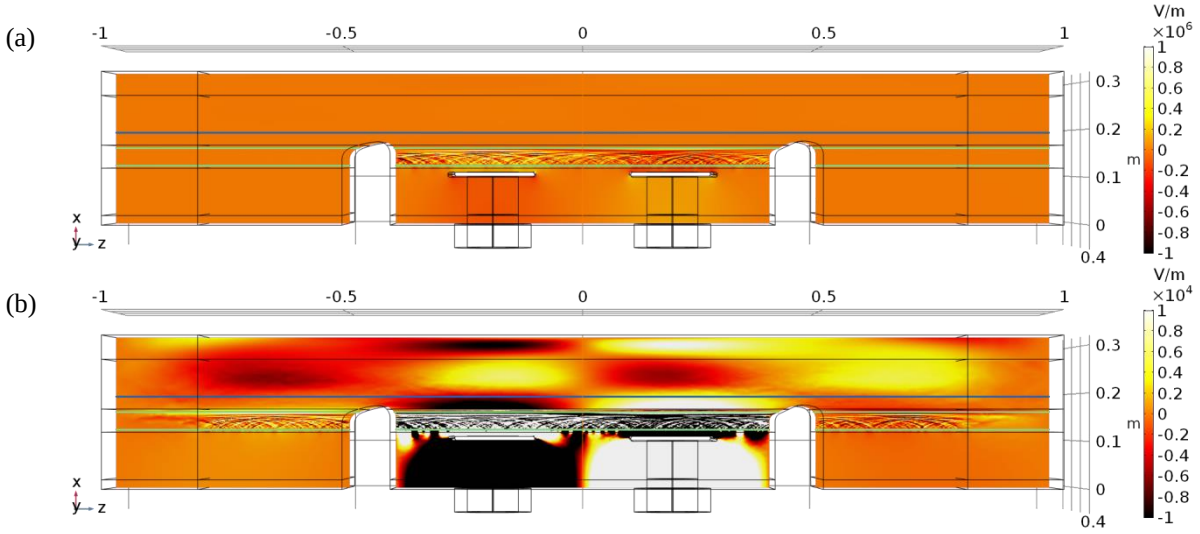

FIGURE 4. (a) E_x distribution in a model with propagating FW and SW, (b) same with shortened color scale range

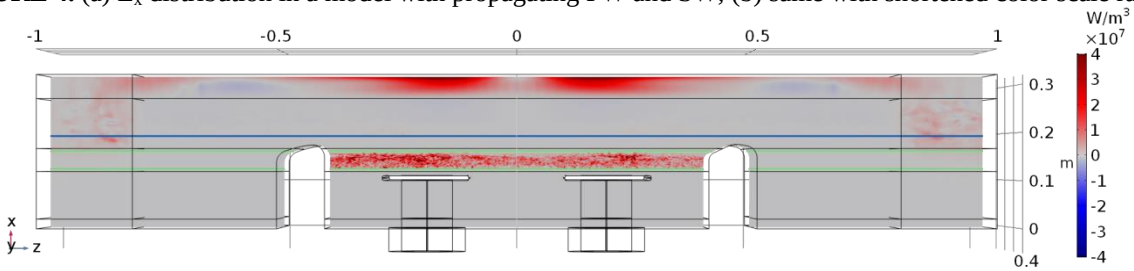

FIGURE 5. Power dissipation density, with spatially separated regions of the SW and the FW absorption

SUMMARY

Advanced methods of the SW RC simulation from [2] applied to tokamak conditions made it possible to include the full realistic density profile (no vacuum layer) into a 3D model of a tokamak ICRF antenna for the first time. The collisional correction is not a purely artificial feature to resolve the LH resonance issue (as was the case with the vacuum layer) but rather a part of the actual physics present in experimental devices that needs to be included in the modeling. The obtained field distribution clearly demonstrates the presence of both propagating SW and FW and represents the experimental ICRF antenna fields more precisely than models which artificially exclude the SW propagation. The collisional absorption of the propagating SW is significant – 9 % of the total coupled power for the considered conditions (very sensitive to the exact conditions). The present model involves some simplifications but its principles can be transferred to full models with toroidal and poloidal plasma and antenna inhomogeneities.

ACKNOWLEDGMENTS

This work has been carried out within the framework of the EUROfusion Consortium and has received funding from the Euratom research and training program 2014-2018 and 2019-2020 under grant agreement No 633053. The views and options expressed herein do not necessarily reflect those of the European Commision.

REFERENCES

1. W. Tierens et al., Nucl. Fusion **59** 046001 (2019)
2. M. Usoltceva et al, Plasma Phys. Control. Fusion (2019)
3. T.H. Stix, *Waves in plasma*, second edition (AIP, 1992)
4. W. Zhang et al., Nucl. Fusion **56** 036007 (2016)
5. H. G. Booker, *Cold plasma waves* (Martinus Nijhoff Publishers, Dordrecht - Boston - Lancaster, 1984)